Please cite the Published Version

Additional Information: This is an Open Access article which appears in Dental Materials, published by Elsevier
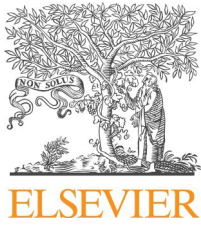
Mechanical behaviour of prosthodontic CAD/CAM polymer composites aged in three food-simulating liquids

Rua S. Babaier[a,b], Julfikar Haider[a,c], Abdulrahman Alshabib[d,e], Nick Silikas[a,*], David C. Watts[a,f,**]

[a] Division of Dentistry, School of Medical Sciences, University of Manchester, United Kingdom
[b] Prosthetic Dental Sciences, College of Dentistry, King Saud University, Saudi Arabia
[c] Department of Engineering, Manchester Metropolitan University, Manchester, United Kingdom
[d] Restorative Dental Sciences, College of Dentistry, King Saud University, Saudi Arabia
[e] Engr. Abdullah Bugshan Research Chair for Dental and Oral Rehabilitation, King Saud University, Saudi Arabia
[f] Photon Science Institute, University of Manchester, United Kingdom

ARTICLE INFO

ABSTRACT

Objectives: This study investigated the effect of ageing in three food-simulating liquids (FSLs) on mechanical properties of three prosthodontic CAD/CAM polymer composites intended for construction of implant-supported frameworks.

Methods: Materials investigated were: (i) a carbon fibre-reinforced composite (CarboCAD 3D dream frame; **CC**), (ii) a glass fibre-reinforced composite (TRINIA; **TR**), and (iii) a reinforced PEEK (DentoKeep; **PK**). Filler contents and microstructural arrangements were determined by thermo-gravimetry and tomography (μ-CT), respectively. Flexural properties (FS and E_f) were measured by 3-point bending (3PB) of 1 mm and 2 mm thick beam specimens. Fracture toughness (K_{IC}) was measured by *single-edge-notched-bending* (SENB). All measurements were made at baseline (dry) and after 1-day and 7-day storage at 37 ℃ in either water, 70 % ethanol/water (70 % E/W) or methyl ethyl ketone (MEK). Failed specimens were examined microscopically. Statistical analyses included four-way ANOVA, two-way ANOVA and multiple Tukey comparison tests ($\alpha = 0.05$). Multiple independent t-tests were performed regarding thickness effects on FS and E_f ($\alpha = 0.05$).

Results: At baseline, the mechanical properties increased in the sequence: PK < TR < CC ($p < 0.001$). FS ranged from 192.9 to 501.5 MPa; E_f from 4.2 to 18.1 GPa; and K_{IC} from 4.9–12.4 MPa.m$^{0.5}$. Fibre-reinforced composites (CC and TR) were significantly stronger than PK. However, all properties of **CC** and **TR** reduced after 1 d storage in 70 % E/W and MEK with FS ranging from 58.6 to 408 MPa; E_f from 1 to 15.4 GPa; K_{IC} from 6.87 to 10.17 MPa.m$^{0.5}$. Greater reductions occurred after 7 d storage. MEK was more detrimental than 70 % E/W and water on fibre-reinforced composites.

---

* Corresponding author.
** Correspondence to: University of Manchester, School of Medical Sciences, Coupland 3 Building, Oxford Road, Manchester M13 9PL, United Kingdom.
 E-mail addresses: nikolaos.silikas@manchester.ac.uk (N. Silikas), david.watts@manchester.ac.uk (D.C. Watts).

Significance: Mechanical properties of each CAD/CAM composite were strongly dependent upon media and ageing. Although the mechanical properties of **PK** were initially inferior, it was relatively stable in all FSLs. All three materials exhibited sufficient mechanical properties at 1 mm thickness, but thicker specimens were more tolerant to ageing.

1.   Introduction

Metal ceramics, previously called porcelain fused to metal, have been the material of choice for fabricating *implant-supported prostheses* (ISP) [1]. However, a paradigm shift to a non-metallic era has resulted in various innovative restorative and prosthetic framework materials such as polycrystalline zirconia [2]. However, because of their great rigidity and mechanical incompatibility with natural oral structures, issues such as vertical bone loss and veneer chipping have arisen [2]. Therefore, demand has increased for biomimetic materials to improve the sustainability of prosthetic treatment. Moreover, advances in CAD/CAM technology, with its controlled production methods, has re-directed research towards *reinforced* polymer-based composites as viable alternatives to conventional prosthetic materials.

Compositional developments have involved combining different matrices with fillers such as ceramic particles or incorporating different fibres such as glass or carbon. These CAD/CAM blocks, often described as *high-performance polymer* (HPP) composites, have been indicated for post and core [3,4] and fixed and removable prostheses [5,6]. Their superior mechanical properties have extended their clinical applications to *implant-supported frameworks* (ISF) [7–11]. Previously, a five-year longitudinal multicentre study assessed the clinical performance of conventionally produced carbon-graphite fibre-reinforced PMMA as ISF [12]. Although these fibre-reinforced composites (FRC) were biocompatible, with good precision and at a reasonable cost compared to metal ISF, their mechanical qualities were inadequate, as the survival rate was only 70 % [12]. In contrast, a recent five-year retrospective clinical study [13] reported comparable cumulative survival rates for ISFs fabricated from reinforced PEEK and titanium (93.1 % and 93.5 %, respectively). The most frequent complication was fracture of the veneer material. However, reinforced PEEK and carbon fibre reinforced composites were associated with significantly lower vertical bone loss as ISF (0.7 and 0.8 mm, respectively) than the titanium group (0.96–1.0 mm) [14].

A few in vitro studies have investigated HPP composites in terms of their load dissipating feature [15–18], biocompatibility [19–21] and mechanical properties in relation to fibre orientation [22,23] or filler content [24]. However, there is a need to monitor mechanical properties of new polymer composites under simulated challenges of the oral environment. The ageing process is complex and involves many interacting variables including chemical, physical, mechanical and thermal variables.

Dental biomaterials are exposed to various liquids induced naturally or absorbed from dietary and oral care products. Ethanol and methyl ethyl ketone (MEK) are two organic solvents, frequently used as food-simulating liquids that have been approved by the US Food and Drug Administration (FDA) [25]. Measuring flexural strength of specimens subjected to accelerated ageing using organic solvents at relatively high concentrations has been established for conventional and reinforced CAD/CAM polymeric composites [26–29]. However, the mechanical behaviour of such polymer composites aged in organic solvents needs more extended investigation. Furthermore, mechanical properties measured in thin sections may assist interpretation of clinical behaviour for cases with limited occlusal space.

The present investigation concerns effects of three *food-simulating liquids (*FSLs) on mechanical properties of three CAD/CAM polymer composite blocks, at two different thicknesses, designed for constructing ISFs. Mechanical properties studied were flexural strength (FS), flexural modulus (E_f) and fracture toughness (K_{IC}) (single-edge-notched-beam) measured by three-point bending. The null hypotheses were as follows:

1. No differences in mechanical properties between three materials, for each thickness, at baseline (dry, without ageing).
2. No differences in FS, E_f, K_{IC} of each material after specimen storage in three media: water, 70 % ethanol/water (70 % E/W) and MEK.
3. No differences in FS, E_f, K_{IC} of each material after specimen storage in the three media for 7 d *compared to* 1 d.
4. No differences in FS and E_f between 1 mm and 2 mm thick specimens.

2.   Materials and methods

2.1.   Study design

A total of 657 specimens were prepared from three CAD/CAM polymer composite blocks (Table 1): *carbon-fibre reinforced composite* (**CC**), *glass fibre-reinforced composite* (**TR**) and *ceramic-filled polyether ether ketone* (**PK**). Specimens were sectioned into plates or beams, as required for each property investigated, using a diamond disc saw (IsoMet 1000 Precision saw, Buhler). The specimens were manually polished with SiC grinding papers: grits P600 and P800 to round off any sharp edges. Specimen dimensions were measured with a digital micrometre (± 0.02 mm) and all specimens were ultrasonically cleaned for five min. **CC** specimens were fired at 80 °C for 2 h, following the manufacturer recommendations, while **TR** and **PK** specimens did not require any firing.

Table 1 – CAD/CAM polymer materials and manufacturer information.				
Code	CAD/CAM Material	Composition	Properties	Manufacturer
CC	CarboCAD 3D Dream frame	Carbon-fibre-reinforced composite	Carbon fibre Epoxy resin of plant origin (Bioresin) No information on composition is available	FS 421 MPa E_f 20.4 GPa	DEI®italia, Italy
TR	TRINIA	Glass fibre-reinforced composite	55–60 % Glass fibre 40–45 % epoxy resin	FS 393 MPa E_f 18.8 GPa K_{IC} 9.7 MPa.mm$^{0.5}$	Bicon Europe, Ltd, Ireland
PK	DENTOKEEP	Ceramic-filled polyetherether ketone	20 % wt TiO_2 80 % wt PEEK	FS 165 MPa E_f 3.8 GPa	NT-Trading, Germany
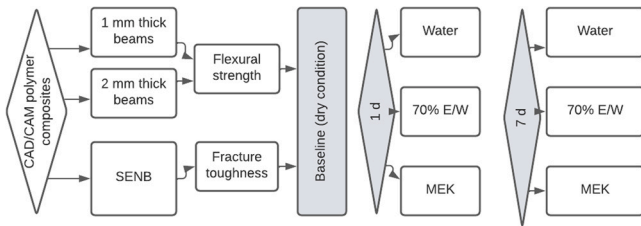
Fig. 1 – Flowchart and ageing groups for the three CAD/CAM materials (N = 210 per material, n = 10 per subgroup).

The flexural strength (FS), flexural modulus (E_f), and fracture toughness (K_{IC}) were measured dry, 24 h after preparation (± 23 °C) (baseline). Then properties were re-measured after 1 d and 7 d storage in three media at 37 °C: water (W), 70 % ethanol/water (E/W), and methyl ethyl ketone (MEK). Fig. 1 presents the distribution of specimens for flexural and fracture toughness tests with three media and two durations both in dry and aging conditions. FS and E_f were measured for both 1 mm and 2 mm thick beams. The supplementary file includes representative images for several experimental steps.

2.2. Filler content and density

The filler content (mass percentage) was measured using the standard ash method (ISO 1172/1996 [30]. Using a calibrated analytic balance (accurate to 0.0001 g)), the mass (mg) of three specimens per material (2 mm × 9 mm × 15 mm) was recorded before and after heating in a furnace at 630 C for 30 min (Programat EP 3000, Ivoclar Vivadent). Specimen dimensions were measured digitally (to 0.01 mm). Average filler contents (wt. %) were calculated via Eq. (1).

$$\text{Filler content (\%)} = (a_2 - a_1) \times 100 \tag{1}$$

where a_1 is the mass of the dry specimen and a_2 is the mass of the ashed specimen.

The density of six specimens from each material was calculated via Eq. (2).

$$\rho = \frac{m}{V} \tag{2}$$

where, m is mass (g) and V is volume (cm^3).

2.3. Micro-CT (µCT) imaging

To examine the structural configuration, one specimen from each material was scanned (dry) (1172 micro-CT; Bruker Skyscan, Belgium). To setup the scanner, 25 kV voltage, 110 A anode current, 1180 ms exposure duration, 4.84 µm image pixel size and 0.4 rotation step for 360° angle were used. To improve signal-to-noise ratio, frame averaging of 4 was applied and to eliminate ring artifacts, random movement of 8 was included. Reconstruction of the projected images was performed using ©N-Recon, (version 1.6.9.4; Bruker Skyscan, Belgium) to produce cross-sectional images. Reconstructed images were saved as 16-bit TIFF files and loaded to ©Dataviewer software (version 1.5.6.2; Bruker Skyscan, Belgium) to examine the 3D datasets.

2.4. Flexural strength and modulus

Specimens (n = 140) from each material were prepared as beams and divided into two groups based on their thickness: 1 mm/2 mm thickness × 18 mm length × 4 mm width. For each thickness, specimens were subdivided into seven groups (n = 10). FS was measured dry, via a universal testing machine (Instron 5965, USA, calibrated 5 kN load cell), and then after storage in three FSLs at 37 °C for 1 d and 7 d. Each beam specimen was measured via three-point bending across a 12 mm span at a crosshead speed of 1 mm/min until fracture, following ISO 6872/2018 [31]. The flexural strength FS (MPa) was calculated via Eq. (3), which is derived on the basis of assumed linear-elastic behaviour:

$$FS = \frac{3FL}{2wh^2} \tag{3}$$

where F was the maximum load (N) at the highest point of each load-deflection curve; L is the span length between supports (mm); w is the specimen width (mm), and h is the height (mm).

The flexural modulus E_f (GPa) was calculated from the slope of the load-deflection curve in the linear region, via Eq. (4), also based on linear-elastic assumptions:

$$E_f = \frac{L^3 F}{4wh^3 d} \tag{4}$$

where d is the deflection (mm).

Table 2 – Filler content and density of CAD/CAM polymer composites.				
Materials	Measured data		Manufacturers' data	
	Density (g/cm^3)	Filler content (wt. %)	Density (g/cm^3)	Filler content (wt. %)
CC	1.34 (0.01)[a]	42.48 (0.39)[a]	1.25–1.33	No information
TR	1.63 (0.04)[b]	55.83 (1.4)[b]	1.68	55–60
PK	1.45 (0.07)[c]	21.34 (1.56)[c]	1.3–1.5	20
Different superscript letters indicate significant differences between materials ($p = 0.0001$).				

2.5. Fracture toughness

Seventy beam specimens per material (18 mm × 4 mm × 3 mm) were sectioned and divided into 7 subgroups (n = 10). A *single-edge-notched-beam* (SENB) methodology was followed for miniature 3PB tests [32]. K_{IC} was measured dry and then after storage in three FSLs at 37 °C for 1 d and 7 d. Fracture toughness is an intrinsic material property thus not influenced by specimen geometry nor the testing methodology but is affected by internal flaw features [33].

A sharp notch was cut in the centre of each beam using a diamond disc and a slow-speed handpiece fixed to a positioning device. Each specimen was secured in a metal holder, with the 3 mm wide surface upwards, on a sliding surface to create a standardised 1.8 ± 0.2 mm notch depth. A razor blade embedded in diamond paste was placed at the base of the notch to create an initial crack. Then, the beams were removed and cleaned with distilled water in an ultrasonic bath for 10 min. Fracture toughness (K_{IC}) was measured at 23 ± 1 °C by three-point bending with a universal testing machine (Instron 5965, MA, USA), according to ISO 10477/2020 [34] and ASTM D5045–14 [35]. A calibrated 5 kN load cell, aligned at the centre of a 12 mm span, recorded loads at a crosshead speed of 1 mm/min, until fracture occurred. Measurements of the crack length were recorded by a light microscope at ×50 magnification.

Fracture toughness K_{IC} (MPa.m$^{0.5}$) was calculated via Eq. (5), which assumes *linear-elastic* material behaviour:

$$K_{IC}\left[\frac{FL}{BW^{1.5}}\right]Y \tag{5}$$

F is the maximum load to fracture (N); *L* is the span length between the supports (m); *B* is the specimen width (m), *W* is the height (m), and *Y* is a geometrical function calculated by Eq. (6) where *a* is the crack length (m) and *w* is the height (m):

$$Y = \left[2.9\left(\frac{a}{w}\right)^{1/2} - 4.6\left(\frac{a}{w}\right)^{\frac{3}{2}} + 21.8\left(\frac{a}{w}\right)^{\frac{5}{2}} - 37.6\left(\frac{a}{w}\right)^{\frac{7}{2}} + 38.7\left(\frac{a}{w}\right)^{\frac{9}{2}}\right] \tag{6}$$

2.6. Microscopic imaging and fracture analysis

Three specimens of **CC**, **TR**, and **PK**, from each ageing group, were examined after 3PB at ×50 and ×100 magnification using a light microscope (Hirox Digital Microscope KH-7700, USA). An additional representative specimen from each 7-d storage group was selected for SEM imaging after the 3PB and SENB. Debris from the specimens were cleaned using an ultrasonic bath for 5 min. The specimens were dehydrated in a series of ascending mixtures of ethanol (70 %, 80 % and 100 %, respectively) before applying a thin gold coating by a sputtering technique. The fracture site of each specimen was imaged in backscattered electron mode at 10 kV (SEM, JSM-6610 LV, JOEL Company, Tokyo, Japan).

2.7. Statistical analysis

Data were analysed using statistical software (SPSS 22.0; IBM SPSS Statistics Inc., Chicago, IL, USA). Normality and homogeneity of variance of the data were confirmed using the Shapiro-Wilk and Levene's tests, respectively. At baseline, differences in mechanical properties (FS, E_f, K_{IC}) between the materials were investigated using one-way ANOVA.

2.7.1. Flexural strength and modulus

Four-way ANOVA was performed to investigate interactions between: materials, storage media, thickness, with FS and E_f. For each thickness group, three-way ANOVA and one-way ANOVA were used followed by Tukey post hoc tests ($\alpha = 0.05$), to detect any differences between the materials within each ageing medium in terms of storage duration ($\alpha = 0.05$). Multiple independent t-tests were performed to investigate the effect of thickness on FS and E_f ($\alpha = 0.05$).

2.7.2. Fracture toughness

Three-way ANOVA was performed to investigate interactions between materials and storage media with fracture toughness. One-way ANOVA was followed by Tukey post hoc tests ($\alpha = 0.05$), to detect any differences between the materials within each ageing medium in term of storage duration ($\alpha = 0.05$).

3. Results

3.1. Filler content and density

Table 2 presents the mean (SD) density (n = 6) and filler content (wt. %) (n = 3) compared to the manufacturers' data. **TR** specimens had higher density and filler content followed by **CC** and **PK** ($p = 0.0001$).

3.2. Micro-CT imaging

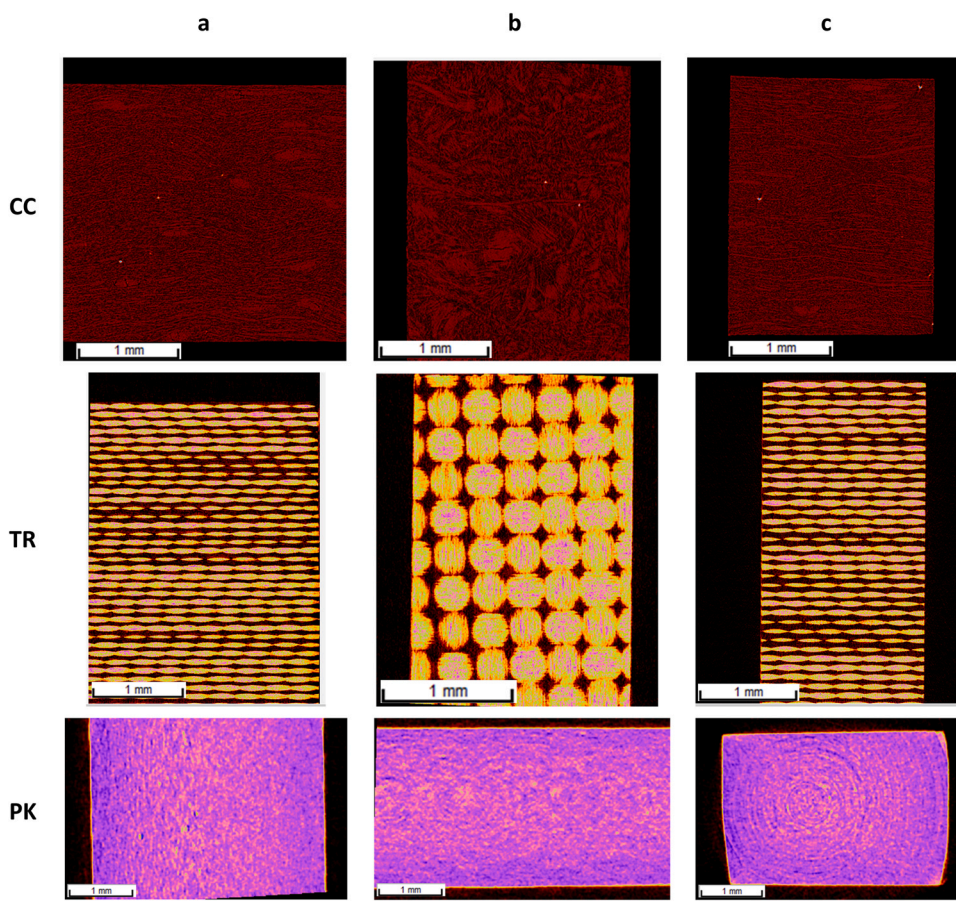The μCT images representing coronal, sagittal and transverse aspects of one dry specimen from each material

Fig. 2 – Representative μCT images of CAD/CAM specimens (CC, TR, and PK) in (a) coronal (b) sagittal, and (c) transverse planes.

showing the differences in fibre orientation between the FRC blocks. In **CC**, carbon fibres were arranged in a random 3D network whereas in **TR**, the glass fibres were layered in two planes (Fig. 2). A homogeneous microstructure was observed in **PK**.

3.3. Flexural strength and modulus

Fig. 3. presents the baseline FS and E_f for the CAD/CAM specimens in terms of thickness. FS and E_f ranged from 192.9 to 501.5 MPa and from 4.2 to 18.2 GPa, respectively, in the
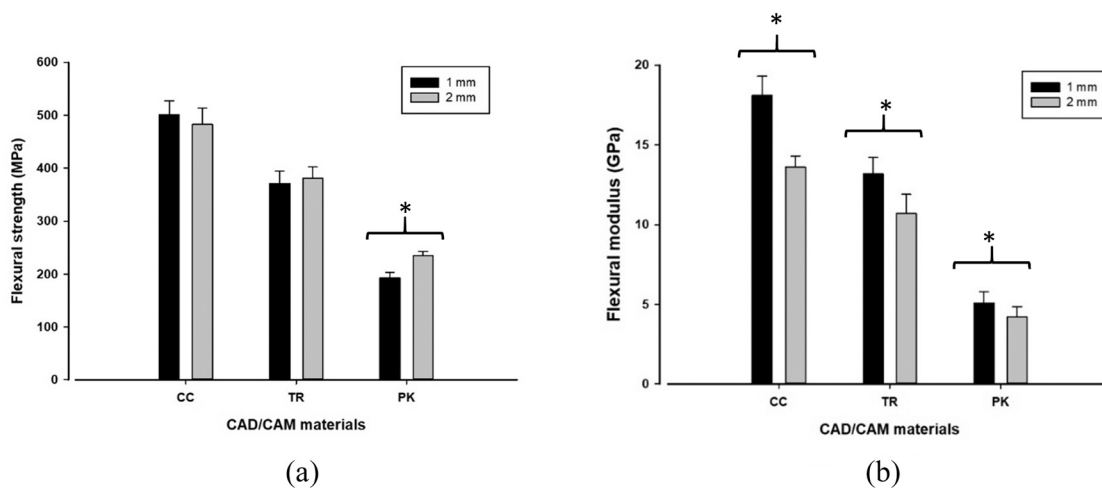

Fig. 3 – Flexural strength (a) and flexural modulus (b) of CAD/CAM specimens (CC, TR and PK) at baseline for 1 mm and 2 mm thickness. Asterisks indicate statistically significant differences ($p < 0.05$).

following ascending sequence: PK < TR < CC ($p < 0.001$). The impact of specimen thickness on FS varied for each material with no significant differences for **TR** and **CC** specimens ($p = 0.07$ and $p = 0.154$, respectively). However, the 2 mm thick **PK** specimens had higher FS than at 1 mm thick ($p < 0.001$). The calculated elastic moduli for 1-mm specimens of all materials were lower than for the corresponding 2-mm specimens ($p < 0.001$).

Tables 3 and 4 present the effect of ageing media and duration on FS and E_f for the CAD/CAM materials. The FS data are plotted in Fig. 4.

Numerical results suggest slightly different mechanical (FS and E_f) for 2 mm and 1 mm thick specimens, after ageing in water and 70 % E/W. 1-mm thick **CC** specimens exhibited somewhat higher *(apparent) elastic moduli* than 2 mm specimens after 1 d storage in 70 % and MEK. This phenomenon is considered below in the Discussion. However, after 7 d in MEK, both thicknesses 'levelled' with nearly 72 % strength loss. Aged PK specimens, on the other hand, demonstrated relative stability, with minor but significant variations between 1- and 2-mm thicknesses. For simplicity, results of the 2-mm thickness specimens only are presented in the following text.

After ageing, both FS and E_f decreased significantly for **CC** and **TR** specimens in 70 % E/W and MEK ($p = 0.0001$). In water, **CC** and **TR** had minimal reductions in FS after 7 d (~1 %, $p = 0.16$), whereas **PK** specimens showed more reduction after 1 day (22 %) followed by a slight recovery after 7 d with statistical significance ($p = 0.001$).

MEK caused progressive deterioration in the **CC** and **TR** specimens irrespective of their thickness ($p < 0.05$). After 24 h storage in MEK, FS reduced by 33 % and 64 % for **CC** and **TR** specimens, respectively. There were no significant differences in FS between **PK** specimens stored in water and MEK, irrespective of storage duration. Also, **PK** specimens stored in MEK had slightly higher moduli than specimens stored in 70 % E/W ($p = 0.012$).

3.4. Fracture toughness

Table 5 presents the SENB fracture toughness (K_{IC}) data at baseline and after storage in FSLs and the results are graphically illustrated in Fig. 5. For reasons explained in the Discussion, these K_{IC} data might, conservatively, be regarded as *apparent fracture toughness*. Baseline K_{IC} measurements widely ranged from 5 to 12 $MPa.m^{0.5}$ in the following ascending sequence: **PK** < **TR** < **CC** ($p < 0.001$).

After 1-day storage in water and 70 % E/W, **CC** specimens had a slight reduction in K_{IC} ($p = 0.001$), then specimens maintained a comparable resistance after 7 days. While **TR** specimens showed no significant changes in the two media nor durations ($p = 0.07$).

MEK caused progressive deterioration in **CC** and **TR** causing nearly 87 % reduction in their resistance to fracture propagation after 7-day storage ($p < 0.001$). In contrast, MEK increased the mean K_{IC} measurements for **PK** by 20 %.

Although 7-day ageing in water and 70 % E/W caused around 40 % increase in the mean K_{IC} measurements for **PK**, the material was relatively stable across all three media and exposure durations.

Table 3 – Flexural strengths (MPa) of two thicknesses of CAD/CAM specimens after storage at 37 °C in water, 70 % ethanol/water, and MEK for 1-day and 7-day (n = 10 per subgroup), calculated according to Eq. 3

Thickness (mm)	Material	FS (MPa) Baseline	FS (MPa)-Storage media and time					
			1d			7d		
			Water	70 % E/W	MEK	Water	70 % E/W	MEK
1	CC	501.5 (25.8)^A,1	494.1 (53.4)^a,A,1	408 (39)^b,A,2	203.8 (12.6)^c,A,2	447.1 (43.4)^a,A,2	268 (19.6)^b,A,3	137.5 (15.3)^c,A,3
	TR	371.5 (23.2)^B,1	339 (25.8)^b,B,2	321.2 (18.9)^b,B,2	58.6 (13.7)^e,B,2	365.9 (38.3)^a,B,3	263.3 (26.4)^b,A,3	12.6 (0.6)^c,B,3
	PK	192.9 (10)^C,1	152.7 (5.4)^b,C,2	156.6 (8.7)^b,C,2	166.9 (8.7)^c,C,2	179.5 (10)^a,C,3	157.6 (8.6)^b,B,2	176.7 (16.8)^a,C,2
2	CC	482.5 (30.9)^A,1	480.4 (27.9)^a,A,1	474.1 (42.6)^a,D,2	325.4 (36.6)^b,D,2	458.6 (26.4)^a,A,1	415 (23.3)^b,C,2	136.6 (6.2)^c,A,3
	TR	381.6 (20.5)^B,1	378.8 (19)^a,D,1	333.4 (27.1)^b,B,2	139.3 (16)^c,E,2	348.7 (66.1)^a,B,1	305.9 (28.6)^a,D,2	32.8 (3.6)^b,D,3
	PK	234.9 (8.5)^D,1	182.4 (9.8)^a,b,E,2	177.7 (9.1)^a,E,2	191.7 (11.4)^b,F,2	199.2 (14.1)^a,D,3	176.1 (19.3)^b,E,2	204.5 (15.2)^a,E,2

In each column, different superscript uppercase letters indicate significant differences between materials ($p \leq 0.05$). For each row, different superscript lowercase letters indicate significant differences between ageing media within a storage time (1d and 7d, independently) ($p \leq 0.05$). For each row, different numbers indicate significant differences between exposure time (baseline, 1d, and 7d) within one single storage medium ($p \leq 0.05$).

Table 4 – Flexural modulus (GPa) of two thicknesses of CAD/CAM materials after storage at 37 °C in water, 70 % ethanol/water, and MEK for 1-day and 7-day (n = 10 per subgroup), calculated according to Eq. 4

Thickness (mm)	Material	E_f (GPa) Baseline	E_f (GPa)-Storage media and time					
			1d			7d		
			Water	70 % E/W	MEK	Water	70 % E/W	MEK
1	CC	18.2 (1.2)[A,1]	19.8 (2)[a,A,1]	15.4 (1.9)[b,A,2]	3.4 (1.3)[c,A,2]	18.5 (1.6)[a,A,1]	9.3 (1.)[b,A,3]	2.3 (0.3)[c,A,2]
	TR	13.2 (1)[B,1]	12.5 (0.8)[a,B,2]	11.5 (0.6)[b,B,2]	1 (0.2)[c,B,2]	14.2 (1.6)[a,B,2]	9.3 (1.2)[b,A,3]	0.0[c,B,3]
	PK	5.1 (0.7)[C,1]	3.7 (0.5)[a,C,2]	3.8 (0.3)[a,C,2]	3.9 (0.3)[a,A,2]	4.8 (0.3)[a,C,1]	3.7 (0.4)[b,B,2]	3.7 (0.9)[b,C,2]
2	CC	13.6 (0.7)[D,1]	13.5 (0.6)[a,D,1]	12.4 (0.7)[b,D,2]	6.4 (0.8)[c,C,2]	13.2 (0.6)[a,D,1]	9.9 (1.1)[b,A,3]	0.9 (0.3)[c,D,3]
	TR	10.7 (1.2)[E,1]	9.9 (0.2)[a,E,1]	9.2 (0.4)[b,E,2]	2.1 (0.3)[c,D,2]	10.3 (1.7)[a,E,1]	7.7 (0.6)[b,C,3]	0.5 (0.2)[c,D,3]
	PK	4.2 (0.6)[F,1]	3.6 (0.4)[a,C,2]	3.6 (0.2)[a,C,2]	3.8 (0.1)[a,A,1]	4.4 (0.2)[a,F,1]	3.1 (0.5)[b,E,2]	4.2 (0.4)[a,C,1]

In each column, different *superscript uppercase letters* indicate significant differences between materials ($p \leq 0.05$).
For each row, different *superscript lowercase letters* indicate significant differences between ageing media within a storage time (1d and 7d, independently) ($p \leq 0.05$). For each row, different *numbers* indicate significant differences between exposure time (baseline, 1d, and 7d) within a storage medium ($p \leq 0.05$).

3.5. *Microscopic imaging and fracture analysis*

Representative images of the CAD/CAM specimens after three-point bending are presented in Figs. 6–8. All **PK** specimens bent without signs of fracture in all ageing groups. In comparison, **CC** and **TR** specimens showed a mix of complete and incomplete fracture modes in water and 70 % E/W storage media. In MEK, more bending was seen with interlaminar failure and fibre waviness (Fig. 6). Also, MEK caused yellowish staining in **TR** and **PK** specimens while 70 % E/W caused surface changes and pitting on **PK**. Figs. 7 and 8 show protruding fibres at the fracture area of **CC** and **TR** specimens following FS and SENB measurements.

4. Discussion

4.1. *General trends*

The three reinforced CAD/CAM polymer composites designed for prosthetic frameworks, were significantly different in their mechanical properties, namely, flexural strength (FS), flexural modulus (E_f) and fracture toughness (K_{IC}). Storage media and exposure time had a substantial impact on the properties of each material, with few exceptions ($p < 0.001$).

In the case of flexural properties, these were determined for both 1-mm and 2-mm thick specimens, applying Eqs. 3 and 4, respectively, to calculate FS and E_f. Changing material thickness produced greater *apparent differences* in their elastic moduli than in their strength. These standard equations are derived on the assumption of perfect *linear elastic* behaviour. Ideally this should 'normalize out' the resultant quantities, so that they are size-invariant. The fact that moderate differences were apparent between some 1-mm and 2-mm specimen groups (of the same material) suggests that those materials were *not* 100 % linear elastic. Where polymeric matrices are involved, this is not an unusual phenomenon, as is apparent – for example – in compressive creep measurements. Furthermore, the fracture toughness – calculated via Eq. 5 – is also derived under the assumptions of *linear elastic*

fracture mechanics (LEFM). Nevertheless, LEFM can accommodate *a certain amount of plastic deformation* at the advancing crack tip.

At baseline, FS, E_f and K_{IC} for the fibre-reinforced composites (**CC** and **TR**) were significantly higher than for ceramic-filled PEEK ($p < 0.05$). However, after storage in three FSLs, considerably greater changes were recorded in **CC** and **TR** compared to **PK**, especially following MEK and 70 % E/W ageing. Exposure duration showed variation in impact on mechanical properties of the three materials. However, **PK** was relatively stable under different ageing conditions. Results suggested *apparent* favourably high mechanical properties for **CC** and **TR** at 1-mm thickness but were *apparently* less tolerant to solvent storage than their 2-mm counterparts. Therefore, null hypotheses 1 and 2 were rejected but were only partially rejected for NH 3 and 4 on the effects of thickness and storage duration.

4.2. *Microstructural composition and configuration*

Multiple variables within the composition and microstructure play a role in the resultant mechanical properties such as filler type, content, fibre characteristics and arrangement within the polymer matrix, bonding quality at the filler-matrix interface and the composite fabrication technique [26,36].

In this study, two materials were fibre-reinforced: (i) **CC**, composed of multidirectional carbon fibres randomly arranged within bio-epoxy resin [14,37], and (ii) **TR,** composed of woven fibreglass sheets aligned in multiple layers within epoxy resin [22]. The third material, **PK** was a thermoplastic polyether ether ketone (PEEK) polymer filled with ceramic filler particles (titanium oxide 20 wt. %) [15]. The differences in matrix, filler and filler arrangements explain the variability in their mechanical behaviour.

The (wt. %) filler contents might contribute to the differences apparent in their FS, E_f, and K_{IC}. **CC** and **TR** (43 wt. % and 56 wt. %, respectively) initially showed superior properties to **PK** (21 wt. %). Generally, higher filler content (wt. %) in different types of **PK** are associated with harder, stronger and
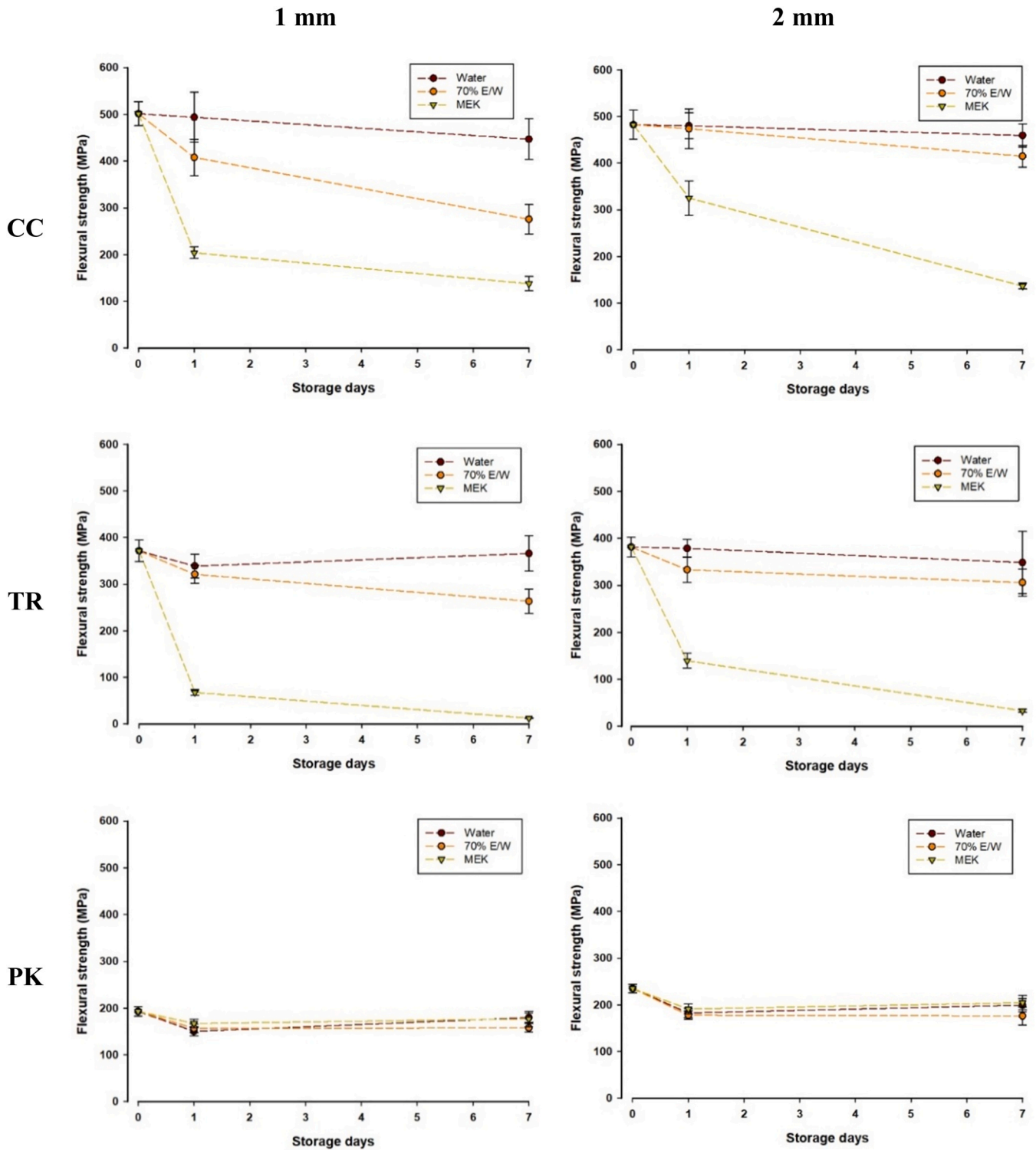
1 mm

2 mm

Fig. 4 – Flexural strength (MPa) of 1 mm and 2 mm thick CAD/CAM composites (CC, TR, and PK) stored in FSLs at 37 °C for 1 day and 7 days. Note the relative stability of PK specimens.

stiffer materials [15,38]. In contrast, in conventional materials with filler content exceeding 55 vol. %, K_{IC} may reduce due to either higher fibre content or poor bonding between fibres and the matrix [39,40]. Nevertheless, this reduction might not be true for materials created via high-temperature and high-pressure (HT-HP) fabrication technology. CAD/CAM methodology was a breakthrough for FRCs, minimising flaws and voids with higher degrees of conversion [6,41,42]. Machined blocks led to fewer complications with handling higher fibre content as encountered in conventional FRCs [20].

Table 5 – SENB Fracture toughness (MPa.m$^{0.5}$) of CAD/CAM specimens after storage at 37 °C in water, 70 % ethanol/water, and MEK for 1-day and 7-day (n = 10 per subgroup), calculated according to Eq. 5

Material	K_{IC} Baseline	Storage media and time					
		1d			7d		
		Water	70 % E/W	MEK	Water	70 % E/W	MEK
CC	12.4 (1.68)[A,1]	10.61 (0.65)[a,A,2]	10.17 (0.42)[a,A,2]	8.42 (0.24)[b,A,2]	10.34 (0.68)[a,A,2]	9.77 (0.59)[a,A,2]	1.57 (0.25)[b,A,3]
TR	9.78 (0.92)[B,1]	9.87 (0.84)[a,A,1]	9.05 (0.544)[a,B,1]	6.87 (0.70)[b,B,2]	9.39 (0.82)[a,B,1]	8.89 (0.86)[a,B,2]	1.19 (0.09)[b,A,3]
PK	4.98 (0.54)[C,1]	5.96 (0.68)[a,B,2]	6.48 (0.62)[a,C,2]	6.52 (0.55)[a,B,2]	7 (0.77)[a,C,3]	7.01 (0.64)[a,C,2]	6 (0.58)[b,C,2]

For each column, different superscript uppercase letters indicate significant differences between materials ($p \leq 0.05$). For each row, different superscript lowercase letters indicate significant differences between ageing media within a storage time (1d and 7d, independently) ($p \leq 0.05$). For each row, different numbers indicate significant differences between exposure time (baseline, 1d, and 7d) within a storage medium ($p \leq 0.05$).

FRC are distinctive for their anisotropic mechanical properties, depending on the direction of load application. The efficiency of fibre reinforcement, or Krenchel factor (K_f), depends on the average fibre direction where $K_f = 1$ for unidirectional fibres and $K_f = 0.5$ for bidirectional fibres [43–46]. Anisotropic behaviour was apparent in **TR** due to its woven glass-fibres (Fig. 2), theoretically with $K_f = 0.5$ [44]. The measured properties of **TR** differ according to the surface selected for investigation [22,23]. However, in **CC**, the braided fibres were randomly oriented in 3-D. Random 3D fibres have $K_f = 0.2$, leading to a nearly isotropic material; hence, any surface should behave similarly irrespective of the loading direction [45]. A similar polymer matrix, even **CC** with lower fibre content, might display better mechanical properties than **TR**, possibly due to differences in C-fibre arrangements compared to glass fibres. However, other differences must be considered, such as the internal strength of the carbon fibres, different interfacial bonding or the 3D fibre distribution.

4.3. Flexural strength and modulus

The minimum FS required for polymer-based materials indicated for core restorative materials is 80 MPa [47] and for polymeric prosthetic materials is 65 MPa [48]. However, higher strength often facilitates application to biomechanically complex structures such as implant-supported prostheses [33]. The main benefit of polymer-based composites in implant dentistry is their biomechanical compatibility [49], with the natural structures being replaced (cortical bone: 13.7–16.4 GPa [50,51] and dentin: 9–18.6 GPa [52,53]). This biomechanical compatibility results from a combination of sufficient high strength and biomimetic modulus matching.

Baseline data suggested that **TR** and **CC** had adequately high strength (ranging from 372 to 502 MPa, respectively), but lower strengths were found for **PK** (193–235 MPa). Also, elastic moduli for **TR** and **CC** ranged from 11 to 18 GPa (lower than manufacturers' data). Specimen thickness affected the flexural modulus data for all three materials, but this is evidently an artifact, as discussed above.

In two similar studies on **TR**, FS and E_f varied with loading directions from 97 to 406 MPa and from 7 to 17 GPa [22,23]. Therefore, the longitudinal surface was selected for conducting flexural measurements on the **TR** specimens, where the load was applied at 90° to the fibre-alignment, resulting in

higher FS by a factor of 2.5 than the parallel surface [22,23]. Moreover, although this was not our objective, additional **TR** specimens were loaded parallel to the fibre direction. Similarly, FS and E_f (n = 10) were significantly lower than the longitudinal data (96–113 MPa and 7–9 GPa), roughly corresponding to FS and E_f for the epoxy resin itself.

The strength of **CC** specimens, however, is unlikely to be affected by the loading direction because of the random fibres. One study reported a range of 408–500 MPa in 3PB [37]. Random fibres resulted in sufficiently high FS (482.5 MPa) in sections as thin as 1-mm.

FS data for **PK** were within the range of other studies, but E_f varied slightly [54,55]. However, the results were compatible with a recent study on 20 % filled PEEK (202 MPa and 4.15 GPa), which were not affected by 1-d storage in water nor thermocycling for 5000 cycles [56].

Subjecting polymer-based composites to accelerated ageing is likely to degrade mechanical properties [42]. The mechanical behaviour after ageing continued to reflect the microstructural differences between the materials and revealed pronounced differences between the effects of the three FSLs.

Irrespective of thickness, **CC** and **TR** specimens stored in 70 % E/W for one day slightly reduced all mechanical properties but they were relatively comparable after water storage. **CC** and **TR** maintained stable behaviour up to 7 days in water and 70 % E/W. However, 1-day storage in MEK caused them more significant degradation than 70 % E/W.

Mechanical properties of **TR** were significantly lower than for **CC**, with its fibre microstructure being more susceptible to solvent absorption. **PK** was relatively more stable during ageing in all FSLs with a slight yet statistically significant decrease in FS and E_f. **PK** was slightly more affected by 70 % E/W than by MEK.

The flexural properties of the three materials measured dry at baseline and at a minimum thickness of 1 mm, might support their application for prostheses in a clinically limited space. However, the results from storage in food-simulating liquids suggest an entirely different conclusion.

4.4. Fracture toughness

Fracture toughness calculated from SENB data via Eq. 5 assumes *linear elastic behaviour*. This may not hold exactly and
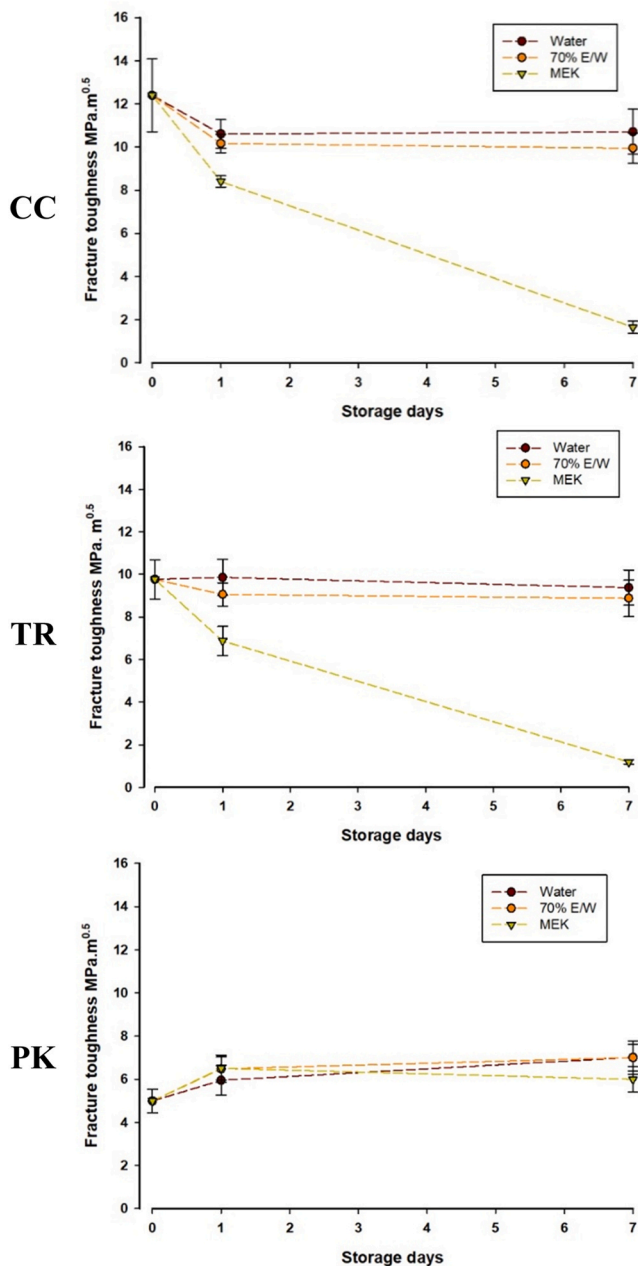
Fig. 5 – Fracture toughness (MPa.m$^{0.5}$) of CAD/CAM composites (CC, TR, and PK) stored in FSLs at 37 °C for 1 day and 7 days.

thus the numerical K_{IC} data might, conservatively, be regarded as *apparent* values. Although there is comparability to some prior data obtained via other methods, those methods may also be subject to the same limitation.

Baseline K_{IC} measurements were higher for **TR** and **CC** (9.8 and 12.4 MPa.m$^{0.5}$, respectively) than for **PK** (5 MPa.m$^{0.5}$) ($p < 0.001$). Higher fracture toughness indicates greater material resistance to cracks initiated from internal or external flaws [36]. Also, the experiments showed that **PK** could dissipate loading forces through elastic-plastic deformation observed as bending before material failure [57].

Filler particles and fibres behave as toughening mechanisms in polymer-based composites by absorbing the stress and deflecting it from the matrix [57]. However, a crack might propagate through the matrix or at the interface, causing complete or partial fibre detachments or delamination, as seen in Fig. 6.

Similar to the present results, the fracture toughness measured by the notchless triangular prism method (NTP) for **TR** was 9 MPa.m$^{0.5}$ in the longitudinal aspect [22]. **CC** specimens exhibited improved resistance to crack propagation compared to **TR** due to its multidirectional fibre arrangement and favourable filler loading (~43 wt. %). Carbon fibres were more effective in absorbing energy. However, **PK** had reduced K_{IC} than the FRC but had equivalent or slightly better fracture toughness than zirconia ceramics (~4 MPa.m$^{0.5}$), which have a totally different structure.

Solvent aging degraded the polymer matrix, fibre-matrix interface or their combination [27]. K_{IC} for **CC** and **TR**, showed similar trends to FS with MEK causing significantly more reduction than water and 70 % E/W. After 7 d of ageing in MEK, K_{IC} for **CC** and **TR** continued to decrease by nearly 87 % from their baseline. However, ageing in water and 70 % E/W for 1 and 7 d were comparable, reflecting relative stability.

In comparison, the 7-d aged **PK** in MEK were higher by 20.5 % from its baseline. The slightly increased fracture toughness in **PK** is probably attributable to a toughening effect due to the plasticisation of the polymer matrix [58]. After 1-d ageing of **PK** in all FSLs, K_{IC} was not significantly different between the three media. Behaviour of **PK** was consistent with previous studies which applied different accelerated ageing protocols such as artificial saliva [55], Ringers solution [54] and thermocycling [56].

4.5. Fractographic analysis

Fractography provides information on the quality of a material and its production through examining different failure modes [59]. Factors including ageing media, temperature, loading rate, and material architecture influence the fracture pattern of polymer composites [58]. The fracture analysis is challenged by the elastic-plastic behaviour of the polymeric materials and the secondary types of failure in FRC, such as delamination and ply splitting [60]. The bonding quality between the fibre and matrix is critical for a crack to initiate or propagate at this interface [58,61]. Moreover, the degree of crystallisation of thermoplastic composites such as **PK**, influenced their mode of failure [54].

CC and **TR** flexural specimens showed mixed patterns of complete and incomplete fracture after storage in water and 70 % E/W groups, irrespective of storage duration. But MEK specimens showed a combination of delamination and fibre waviness, also called impact damage (Fig. 6). The delamination often migrates and grows in multidirectional fibre reinforced composites [58,62], as seen in specimens stored in 70 % E/W and MEK. Also, fibre-bridging was seen at the fractured site preventing complete separation of the fractured beams. The fracture line was not distinct in all **CC** and **TR**, and this might be described as *viscous fracture* as previously suggested for **TR** [22]. At the fracture site (Fig. 7 and Fig. 8), **TR** showed signs of inter- and intra-laminar fractures caused by
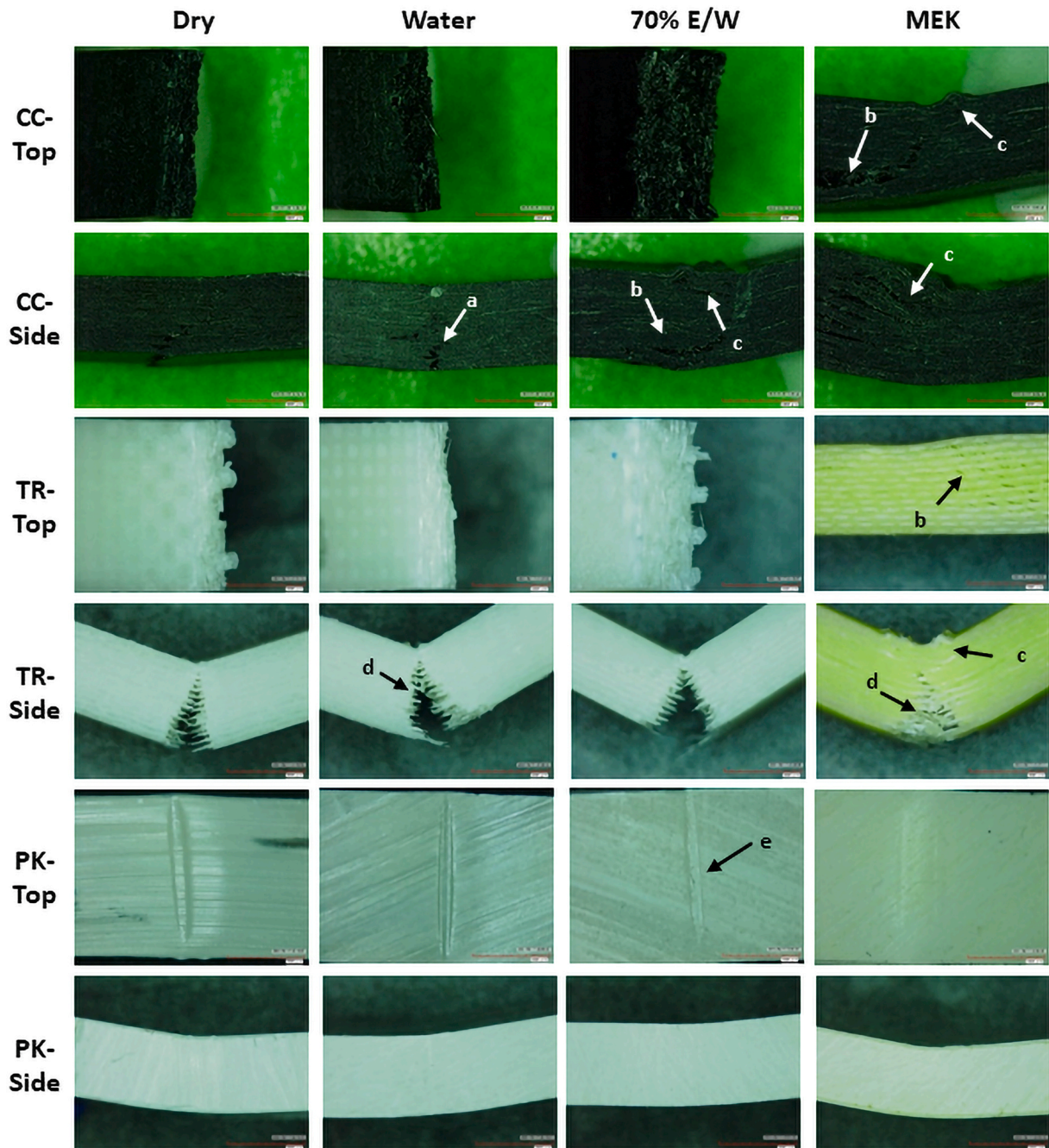
Fig. 6 – Representative images of CAD/CAM specimens (2 mm thickness) subjected to three-point bending after 7-day storage in water, 70 % E/W, and MEK. Incomplete fracture (a), delamination migration (b), fibre waviness (c), fibre-bridging (d) and pitting (e). CC and TR in MEK show side aspects of impact damage.

the interfacial partial debonding of the glass fibres. Whereas **CC** had a translaminar form of failure which involved fibre fracture and micro-buckling.

After solvent storage, all **PK** flexural beams bent upon failure. **PK** aged for 7 d exhibited a greater tendency for matrix ductility compared to 1 d. In contrast, the notched/ SENB **PK** beams fractured catastrophically at comparatively lower loads. SEM images of fractured **PK**, revealed small but multiple surface cracks, voids and hackle radial patterns, like previous studies [63,64]. Understanding different failure

modes for these HPP composites may shed light on their performance throughout clinical service and guide further material development.

4.6. Significance

Although beam-shaped specimens do not simulate the geometry of implant-supported prostheses, their use is necessary for quantitative flexural measurements [33]. Smaller specimens were prepared to accommodate block dimensions
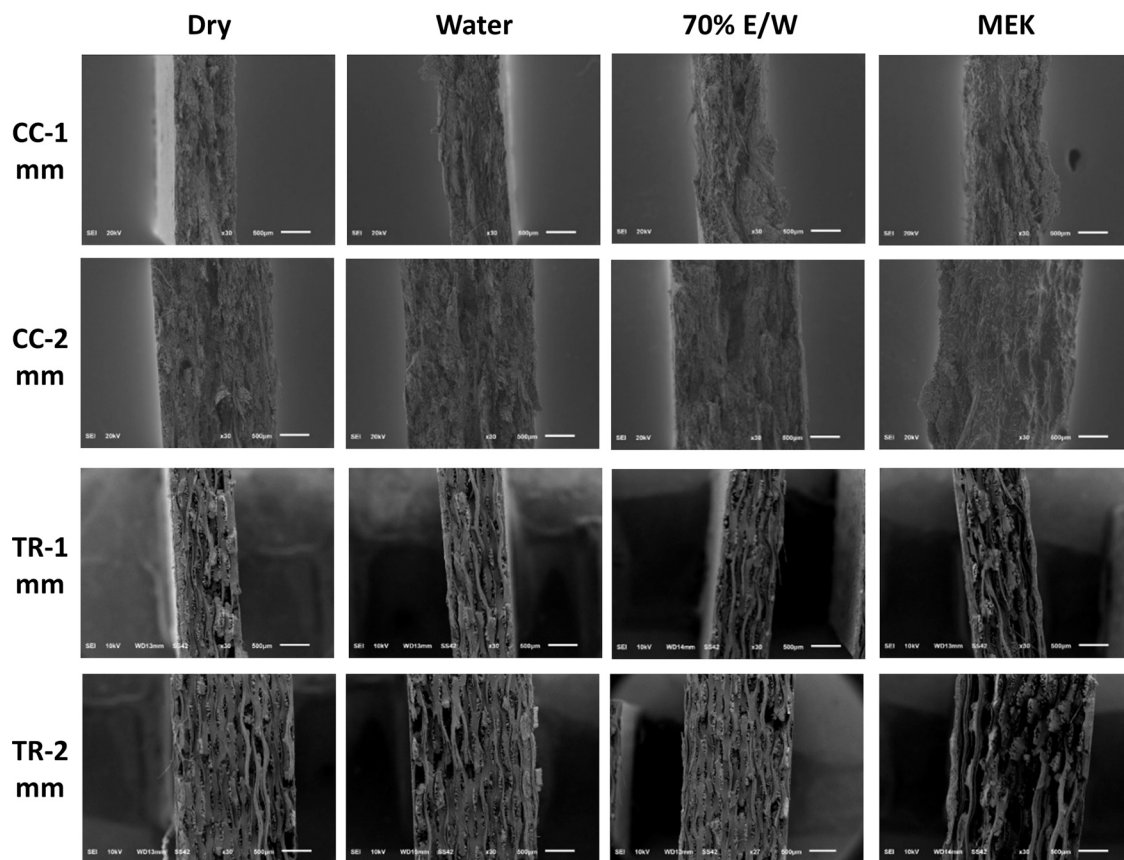
Fig. 7 – Representative SEM images of fractured surfaces of CAD/CAM specimens after 7-day-storage in: water, 70 % E/W, and MEK. Note: PK specimens bent and did not fracture upon 3-point loading.
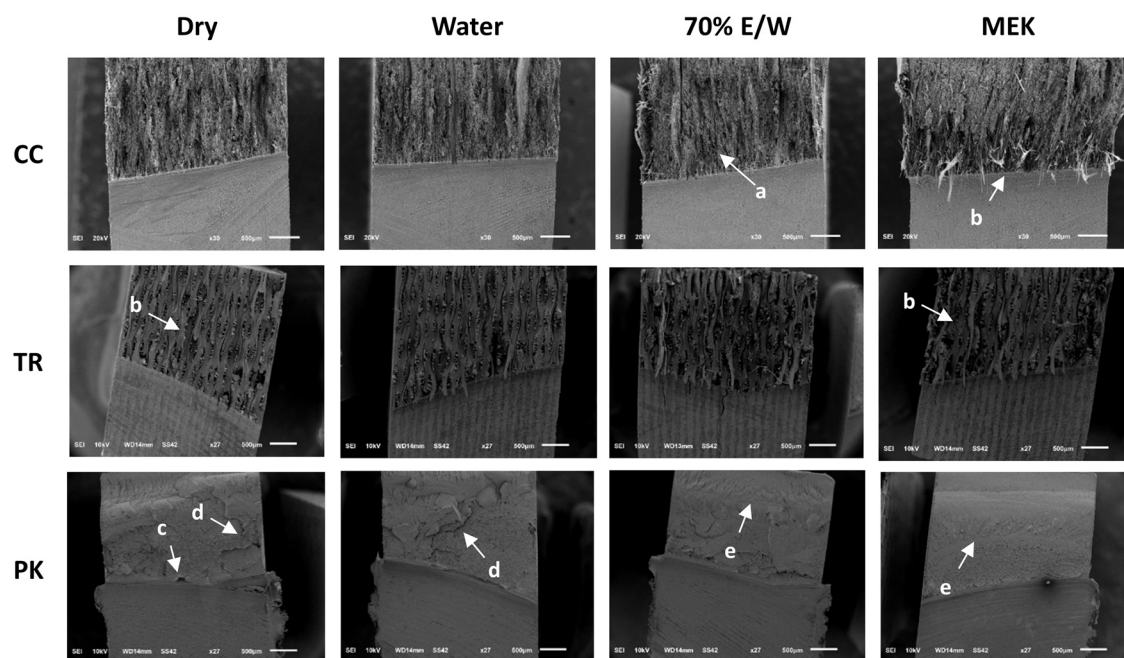

Fig. 8 – Representative SEM images of fractured surfaces of single-edge-notched beam specimens after 7-day storage in water, 70 % E/W, and MEK. Translaminar fracture (a), intra-laminar fracture (b), void (c), cracks (d), and hackle pattern (e).

[32]. This study demonstrates the significant dependence of flexural properties with one form of ageing, chemical storage in three FSLs.

The behaviour of **TR** blocks was dependent on loading direction relative to fibre orientation. Therefore, during prosthesis design, favourable occlusal support must be ensured. However, the multidirectional isotropic fibre arrangement in **CC** seemed more favourable mechanically. **PK** had lower, but more stable, mechanical characteristics than the FRC. Hence, reinforced PEEK for ISF appears beneficial because of its biological and mechanical compatibility, supported by clinical success in the head and spine orthopaedic surgeries [65]. Clinical studies are required to determine long-term performance of implant-supported frameworks fabricated from CAD/CAM HPP composites.

5.   Conclusions

Under dry conditions, fibre-reinforced composites (**CC** and **TR**) showed significantly higher mechanical properties (flexural strength FS, elastic modulus E_f, and (apparent) fracture toughness K_{IC}) than **PK** - the ceramic filled PEEK. However, subjecting the specimens to accelerated ageing in food-simulating solvents resulted in considerable degradation of mechanical properties of the FRCs but to a lesser extent for **PK**.

Dry fibre-reinforced composites were sufficiently strong in 1-mm section. However, their increased strength deterioration in FSLs requires full protection with a veneer material.

Acknowledgement

Appendix A.   Supporting information

Supplementary data associated with this article can be found in the online version at doi:10.1016/j.dental.2022.07.001.

REFERENCES

[1] Wataha JC. Alloys for prosthodontic restorations. J Prosthet Dent 2002;87(4):351–63.

[2] Sailer I, Strasding M, Valente NA, Zwahlen M, Liu S, Pjetursson BE. A systematic review of the survival and complication rates of zirconia-ceramic and metal-ceramic multiple-unit fixed dental prostheses. Clin Oral Implants Res 2018;29(Suppl 16):184–98.

[3] Teixeira KN, Duque TM, Maia HP, Gonçalves T. Fracture resistance and failure mode of custom-made post-and-cores of polyetheretherketone and nano-ceramic composite. Oper Dent 2020.

[4] Hallak AG, Caldas RA, Silva ID, Miranda ME, Brandt WC, Vitti RP. Stress distribution in restorations with glass fiber and polyetheretherketone intraradicular posts: an in silico analysis. Dent Mater J 2022.

[5] Başaran EG, Ayna E, Vallittu PK, Lassila LV. Load bearing capacity of fiber-reinforced and unreinforced composite resin CAD/CAM-fabricated fixed dental prostheses. J Prosthet Dent 2013;109(2):88–94.

[6] Hada T, Suzuki T, Minakuchi S, Takahashi H. Reduction in maxillary complete denture deformation using framework material made by computer-aided design and manufacturing systems. J Mech Behav Biomed Mater 2020;103:103514.

[7] Bonfante EA, Suzuki M, Carvalho RM, Hirata R, Lubelski W, Bonfante G, et al. Digitally produced fiber-reinforced composite substructures for three-unit implant-supported fixed dental prostheses. Int J Oral Maxillofac Implants 2015;30(2):321–9.

[8] AL-Rabab'ah M, Hamadneh Wa, Alsalem I, Khraisat A, Abu Karaky A. Use of high performance polymers as dental implant abutments and frameworks: a case series report. J Prosthodont 2019;28(4):365–72.

[9] Arnold C, Hey J, Schweyen R, Setz JM. Accuracy of CAD-CAM-fabricated removable partial dentures. J Prosthet Dent 2018;119(4):586–92.

[10] Jovanović M, Živić M, Milosavljević M. A potential application of materials based on a polymer and CAD/CAM composite resins in prosthetic dentistry. J Prosthodont Res 2021;65(2):137–47.

[11] Segerström S, Ruyter IE. Effect of thermal cycling on flexural properties of carbon–graphite fiber-reinforced polymers. Dent Mater 2009;25(7):845–51.

[12] Bergendal T, Ekstrand K, Karlsson U. Evaluation of implant-supported carbon/graphite fiber-reinforced poly (methyl methacrylate) prostheses. A longitudinal multicenter study. Clin Oral Implants Res 1995;6(4):246–53.

[13] Wang J, Wu P, Liu H-L, Zhang L, Liu L-P, Ma C-F, et al. Polyetheretherketone versus titanium CAD-CAM framework for implant-supported fixed complete dentures: a retrospective study with up to 5-year follow-up. J Prosthodont Res 2021. JPR_D_20_00142.

[14] Pera F, Pesce P, Solimano F, Tealdo T, Pera P, Menini M. Carbon fibre versus metal framework in full-arch immediate loading rehabilitations of the maxilla–a cohort clinical study. J Oral Rehabil 2017;44(5):392–7.

[15] Schwitalla AD, Spintig T, Kallage I, Müller W-D. Pressure behavior of different PEEK materials for dental implants. J Mech Behav Biomed Mater 2016;54:295–304.

[16] Bergamo ET, Yamaguchi S, Lopes AC, Coelho PG, de Araújo-Júnior EN, Jalkh EBB, et al. Performance of crowns cemented on a fiber-reinforced composite framework 5-unit implant-supported prostheses: in silico and fatigue analyses. Dent Mater 2021.

[17] Stawarczyk B, Thrun H, Eichberger M, Roos M, Edelhoff D, Schweiger J, et al. Effect of different surface pretreatments and adhesives on the load-bearing capacity of veneered 3-unit PEEK FDPs. J Prosthet Dent 2015;114(5):666–73.

[18] Omaish HHM, Abdelhamid AM, Neena AF. Comparison of the strain developed around implants with angled abutments with two reinforced polymeric CAD-CAM superstructure materials: an in vitro comparative study. J Prosthet Dent 2022.

[19] Segerström S, Sandborgh-Englund G, Ruyter EI. Biological and physicochemical properties of carbon-graphite fibre-reinforced polymers intended for implant suprastructures. Eur J Oral Sci 2011;119(3):246–52.

[20] Menini M, Pesce P, Pera F, Barberis F, Lagazzo A, Bertola L, et al. Biological and mechanical characterization of carbon fiber frameworks for dental implant applications. Mater Sci Eng C Mater Biol Appl 2017;70(Pt 1):646–55.

[21] Hahnel S, Wieser A, Lang R, Rosentritt M. Biofilm formation on the surface of modern implant abutment materials. Clin Oral Implants Res 2015;26(11):1297–301.

[22] Suzaki N, Yamaguchi S, Hirose N, Tanaka R, Takahashi Y, Imazato S, et al. Evaluation of physical properties of fiber-reinforced composite resin. Dent Mater 2020;36(8):987–96.

[23] Yasue T, Iwasaki N, Shiozawa M, Tsuchida Y, Suzuki T, Takahashi H. Effect of fiberglass orientation on flexural properties of fiberglass-reinforced composite resin block for CAD/CAM. Dent Mat J 2019;2018–249.

[24] Lümkemann N, Pfefferle R, Jerman E, Sener B. Stawarczyk B. Translucency, flexural strength, fracture toughness, fracture load of 3-unit FDPs, Martens hardness parameter and grain size of 3Y-TZP materials. Dent Mater 2020.

[25] Food and Drug Administration (FDA). Guidelines for chemistry and technology requirements of indirect food additive petitions, Bureau of Foods. Washington, DC, USA: Department of Health EaW; 1976.

[26] Eliades G., Eliades T., Brantley W.A., Watts D.C. Dental materials in vivo: aging and related phenomena: Quintessence Chicago; 2003.

[27] Alshabib A, Algamaiah H, Silikas N, Watts DC. Material behavior of resin composites with and without fibers after extended water storage. Dent Mater J 2021;40(3):557–65.

[28] Bechir F, Bataga SM, Tohati A, Ungureanu E, Cotrut CM, Bechir ES, et al. Evaluation of the behavior of two CAD/CAM fiber-reinforced composite dental materials by immersion tests. Mater (Basel) 2021;14(23).

[29] Alshabib A, Silikas N, Watts DC. Hardness and fracture toughness of resin-composite materials with and without fibers. Dent Mater 2019;35(8):1194–203.

[30] ISO 1172:1996 Textile-glass-reinforced plastics - Prepregs, moulding compounds and laminates - Determination of the textile-glass and mineral-filler content - Calcination methods 1996.

[31] BS EN ISO 6872:2018 - Dentistry. Ceramics. 2018.

[32] Chai H, Wang X, Sun J. Miniature specimens for fracture toughness evaluation of dental resin composites. Dent Mater 2019;35(2):283–91.

[33] Ilie N, Hilton TJ, Heintze SD, Hickel R, Watts DC, Silikas N, et al. Academy of dental materials guidance-resin composites: part I-mechanical properties. Dent Mater 2017;33(8):880–94.

[34] BS EN ISO 10477–2020-Dentistry — Polymer-based crown and veneering materials. 2020.

[35] ASTM I. Standard test methods for plane-strain fracture toughness and strain energy release rate of plastic materials. ASTM D5045–99. 2007.

[36] Ralf J. Dental Resins-Material Science & Technology: Advanced Level. Third ed: tredition GmbH; 2021.

[37] Castorina G. Carbon-fiber framework for full-arch implant-supported fixed dental prostheses supporting resin-based composite and lithium disilicate ceramic crowns: case report and description of features. Int J Periodontics Restor Dent 2019;39(2):175–84.

[38] Lümkemann N, Eichberger M, Stawarczyk B. Different PEEK qualities irradiated with light of different wavelengths: impact on Martens hardness. Dent Mater 2017;33(9):968–75.

[39] Kim KH, Ong JL, Okuno O. The effect of filler loading and morphology on the mechanical properties of contemporary composites. J Prosthet Dent 2002;87(6):642–9.

[40] Fonseca RB, Favarão IN, Kasuya AVB, Abrao MAdS, Luz NFMd, Naves LZ. Influence of glass fiber wt% and silanization on mechanical flexural strength of reinforced acrylics. J Mater Sci 2014;2:11–5.

[41] Stawarczyk B, Eichberger M, Uhrenbacher J, Wimmer T, Edelhoff D, Schmidlin PR. Three-unit reinforced polyetheretherketone composite FDPs: influence of fabrication method on load-bearing capacity and failure types. Dent Mater J 2015;34(1):7–12.

[42] Wendler M, Stenger A, Ripper J, Priewich E, Belli R, Lohbauer U. Mechanical degradation of contemporary CAD/CAM resin composite materials after water ageing. Dent Mater 2021;37(7):1156–67.

[43] Krenchel H. Fibre reinforcement; theoretical and practical investigations of the elasticity and strength of fibre-reinforced materials. 1964.

[44] Vallittu PK. Flexural properties of acrylic resin polymers reinforced with unidirectional and woven glass fibers. J Prosthet Dent 1999;81(3):318–26.

[45] Chong KH, Chai J. Strength and mode of failure of unidirectional and bidirectional glass fiber-reinforced composite materials. Int J Prosthodont 2003;16(2):161–6.

[46] Schwartz M, Fibers and matrices. Composite materials. Vol I: properties. nondestructive testing, and repair princeton. NJ: Prentice Hall; 2012. p. 73–8.

[47] BS EN ISO 4049:2019 - Dentistry. Polymer-based restorative materials. 2019.

[48] BS EN ISO 14577–4:2016. Metallic materials — Instrumented indentation test for hardness and materials parameters — Part 4: Test method for metallic and non-metallic coatings 2016.

[49] Oshida Y, Tuna EB, Aktören O, Gençay K. Dental implant systems. Int J Mol Sci 2010;11(4):1580–678.

[50] Çağlar A, Turhan Bal B, Karakoca S, Aydın C, Yılmaz H, Sarısoy Ş. Three-dimensional finite element analysis of titanium and yttrium-stabilized zirconium dioxide abutments and implants. Int J Oral Maxillofac Implants 2011;26:5.

[51] Zioupos P, Currey JD. Changes in the stiffness, strength, and toughness of human cortical bone with age. Bone 1998;22(1):57–66.

[52] Machnick TK, Torabinejad M, Munoz CA, Shabahang S. Effect of MTAD on flexural strength and modulus of elasticity of dentin. J Endod 2003;29(11):747–50.

[53] Yan J, Taskonak B, Mecholsky JJ. Fractography and fracture toughness of human dentin. J Mech Behav Biomed Mater 2009;2(5):478–84.

[54] Schwitalla AD, Spintig T, Kallage I, Müller WD. Flexural behavior of PEEK materials for dental application. Dent Mater 2015;31(11):1377–84.

[55] Alamoush RA, Silikas N, Salim NA, Al-Nasrawi S, Satterthwaite JD. Effect of the composition of CAD/CAM composite blocks on mechanical properties. Biomed Res Int 2018;2018. 4893143-.

[56] Niem T, Youssef N, Wöstmann B. Influence of accelerated ageing on the physical properties of CAD/CAM restorative materials. Clin Oral Invest 2019.

[57] Niem T, Youssef N, Wostmann B. Energy dissipation capacities of CAD-CAM restorative materials: a comparative evaluation of resilience and toughness. J Prosthet Dent 2019;121(1):101–9.

[58] Greenhalgh E, Hiley M. Fractography of polymer composites: current status and future issues 2008.

[59] Abdulhameed NF, Angus BM, Wanamaker J, Mecholsky JJ. Quantitative fractography as a novel approach to measure fracture toughness of direct resin composites. J Mech Behav Biomed Mater 2020;109:103857.

[60] Kenane M, Benmedakhene S, Azari Z. Fracture and fatigue study of unidirectional glass/epoxy laminate under different mode of loading. Fatigue Fract Eng Mater Struct 2010;33:284–93.

[61] Panek M, Blazewicz S, Konsztowicz KJ. Correlation of acoustic emission with fractography in bending of glass–epoxy composites. J Nondestr Eval 2020;39:1–10.

[62] Davies GAO, Olsson R. Impact on composite structures. Aeronaut J 1968;108(1089):541–63. 2004.

[63] Wei T, Wang J, Yu X, Wang Y, Wu Q, Chen C. Mechanical and thermal properties and cytotoxicity of Al2O3 nano particle-reinforced poly(ether-ether-ketone) for bone implants. RSC Adv 2019;9:34642–51.

[64] Chen F, Gatea S, Ou H, Lu B, Long H. Fracture characteristics of PEEK at various stress triaxialities. J Mech Behav Biomed Mater 2016;64:173–86.

[65] Kurtz SM, Devine JN. PEEK biomaterials in trauma, orthopedic, and spinal implants. Biomaterials 2007;28(32):4845–69.